Ultrasensitive detection of waste products in water using fluorescence emission cavity-enhanced spectroscopy

Joel N. Bixler[a], Michael T. Cone[a], Brett H. Hokr[a], John D. Mason[a], Eleonora Figueroa[a], Edward S. Fry[a], Vladislav V. Yakovlev[a], and Marlan O. Scully[a,b,c,1]

[a]Texas A&M University, College Station, TX 77843; [b]Princeton University, Princeton, NJ 08540; and [c]Baylor University, Waco, TX 76706

Contributed by Marlan O. Scully, March 5, 2014 (sent for review December 1, 2013; reviewed by Peter M. Rentzepis and Vadim Backman)

Clean water is paramount to human health. In this article, we present a technique for detection of trace amounts of human or animal waste products in water using fluorescence emission cavity-enhanced spectroscopy. The detection of femtomolar concentrations of urobilin, a metabolic byproduct of heme metabolism that is excreted in both human and animal waste in water, was achieved through the use of an integrating cavity. This technique could allow for real-time assessment of water quality without the need for expensive laboratory equipment.

water contamination | fluorescence spectroscopy | femtomolar detection

It is axiomatic that the quality of water is essential for human health (1). The increasing worldwide contamination of freshwater systems with thousands of industrial and natural chemical compounds is one of the key environmental problems facing humanity today, where pathogens in water cause more than 2 million deaths annually (2). With more than one-third of the accessible and renewable freshwater used for industrial, agricultural, and domestic applications, pollution from these activities leaves water sources contaminated with numerous synthetic and geogenic compounds (2, 3). In addition, natural disasters can result in large-scale disruptions of infrastructure, resulting in compromised water quality. Diarrheal disease caused from such disasters may be a major contributor to overall morbidity and mortality rates (4). Thus, the cleanliness and safety of public water sources has prompted researchers to look for rapid and sensitive indicators of water quality. Whereas most water filtering systems are quite efficient in removing large-size contaminants, smaller particles frequently pass through. These contaminants are often poorly soluble in water, thus, present in quantities of less than 1 nM. Here, we demonstrate femtomolar detection of urobilin, a biomarker found in human and animal waste in water.

Modern analytical tools have become extremely efficient in the detection and analysis of chemical compounds. For example, liquid chromatography coupled with detection by tandem mass spectrometry has been commonly used for detection of trace pharmaceuticals and other wastewater-derived micropollutants (5). Although such methods are very powerful in identifying trace pollutants, cost prohibits their widespread use by environmental researchers and, most importantly, prevents real-time analysis of water quality (6). Other techniques using bench top gas chromatography–mass spectrometry have also been demonstrated as viable methods for detection of basic pharmaceuticals with reduced cost (7). Despite this, these methods are still cost prohibitive, can hardly be used in field studies, and are unlikely to ever be used for real-time quality control.

In addition to pharmaceutical and other synthetic pollutants such as pesticides, animal and human waste (i.e., feces, urine) is an enormous source of water contamination that can be found in both recreational and source waters. These discarded products, when released into water, can carry a variety of diseases such as polio, typhoid, and cholera (8). In extreme cases pollution of an ecosystem can result in environmental crises, such as devastation to the aquatic population, red-tide blooms, as well as beach closings. Molecular methods based on polymerase chain reactions are commonly used to monitor viral, bacterial, and protozoan pathogens in wastewater (9). Microbiological indicators such as fecal coliforms, *Escherichia coli* and *Etherococci*, are the indicators most commonly used to analyze and evaluate the level of fecal contamination. However, the suitability of these indicators has been questioned (10), and it takes a substantial time from the extraction of water sample for analysis to the moment when the results are ready.

An alternative indicator that has been shown to be helpful in detection of waste in water supplies is urobilin (11). Urobilin is one of the final byproducts of hemoglobin metabolism, and is excreted in both the urine and feces of many mammals, including humans and common livestock (cows, horses, and pigs) (12). In addition, as urobilin can be indicative of disease such as hepatic dysfunction, or jaundice, an ultrasensitive technique for detection and quantification of this biomarker in solution has both diagnostic and environmental applications.

Urobilin detection in solution has previously been demonstrated using the formation of a phosphor group from the combination of urobilins and zinc ions (13). Normal heme catabolism results in the production of bilirubin, a red product, which is then broken down into two end products, stercobilin, the bile pigment found in fecal material, and urobilin, the yellow pigment found in urine. Both urobilin and stercobilin have been shown to be viable biomarkers for detection of fecal pollution levels in rivers (14).

Fluorescent detection of urobilin in urine has been demonstrated based on Schlesinger's reaction in which an urobilinogen–zinc chelation complex exhibits a characteristic green fluorescence when excited by blue light (15). Methods for detection of urobilinoids using high-performance liquid chromatography with a reversed-phase column and an ultraviolet detector have also been

Significance

Clean water is paramount to human health. Contaminants, such as human waste products in drinking water, can result in significant health issues. In this article, we present a technique for detection of trace amounts of human or animal waste products in water. This technique could allow for real-time assessment of water quality without the need for expensive laboratory equipment.

Author contributions: J.N.B., E.S.F., V.V.Y., and M.O.S. designed research; J.N.B., M.T.C., B.H.H., J.D.M., and E.F. performed research; J.N.B., M.T.C., B.H.H., J.D.M., and V.V.Y. analyzed data; and J.N.B., M.T.C., B.H.H., J.D.M., E.S.F., V.V.Y., and M.O.S. wrote the paper.

Reviewers: P.M.R., University of California, Irvine; V.B., Northwestern University.

The authors declare no conflict of interest.

Freely available online through the PNAS open access option.

[1]To whom correspondence should be addressed. E-mail: scully@tamu.edu.

presented (16); however, the initial sensitivity of this method proved insufficient for clinical analysis. Miyabara and coworkers reported an increase in detection sensitivity of this methodology, but only to detection levels of 1.5 nM (13), where efficient excitation and collection of the fluorescent signal remained the limiting factor. Traditional epiillumination fluorescence spectroscopy systems use an objective lens to focus excitation light into the sample and collect the fluorescence emission. In such a configuration, the signal generated is limited to the focal volume of the optics. In addition, the generated signal is diffusive in nature; only a small fraction of the total emitted light is collected. Because only a small volume of a sample can be probed at any given time with such a configuration, detection of subnanomolar concentrations remains difficult as these measurements are akin to single molecule detection. Thus, a method that could allow for probing a larger volume of a sample while also providing means for collecting more of the fluorescence emission could greatly enhance the ability to detect subnanomolar concentrations of urobilin.

Materials and Methods

To achieve both of these goals, we use a custom integrating cavity to enhance both excitation and collection efficiency. Integrating cavities, especially spherical cavities, are commonly used to measure the total radiant flux from a source, as a means to generate uniform illumination, and as pump cavities for lasers (17). In addition to this, such devices have been shown to be a powerful tool for the spectroscopy of weakly absorbing materials (18). Here, we present an application for such cavities: the enhancement of both the excitation and collection of fluorescent emission. Due to the nearly Lambertian behavior of the cavity walls, an isotropic field is created inside the cavity, allowing for fluorescence excitation of the entire volume of any sample placed inside the cavity. In addition, the high reflectivity of the cavity walls leads to very large effective optical path lengths inside the sample region of the cavity. To demonstrate this concept we can consider the following result by Fry et al. in ref. 17. The average distance between reflections $\bar{d}$ inside an integrating cavity of arbitrary geometry can be expressed as

$$\bar{d} = 4\frac{V}{S}, \quad [1]$$

where V is the cavity volume and S is the surface area. The average number of reflections for a given photon inside a cavity of reflectivity ρ is simply $-1/\ln(\rho)$. Thus, we can express the average effective path length L inside the cavity as

$$L = n\bar{d} = -\frac{4}{\ln\rho}\left(\frac{V}{S}\right) \approx \frac{4V}{S(1-\rho)}, \quad [2]$$

where the final approximation is valid when ρ is close to unity.

To experimentally determine the reflectivity of the cavity, a cavity ring-down measurement is used (18–20). This involves sending a temporally short pulse of light into the cavity and measuring the exponential decay of the pulse inside the cavity over time. For an empty cavity the decay constant τ is related to the cavity reflectivity by the well-known relation

$$\tau = -\frac{1}{\ln\rho}\left(\frac{\bar{d}}{c}\right), \quad [3]$$

where c is the speed of light. In this study a 10-ns pulse from a frequency-doubled neodymium-doped yttrium aluminum garnet laser was launched into the cavity via an optical fiber. The decay, or "ring-down" signal, is sampled with another optical fiber, and detected with a photomultiplier tube (PMT). Fig. 1 shows the input laser pulse, the output decay curve, and a fit to that curve. The fit yields a decay constant of 98.14 ns. Using Eq. **3**, this gives a cavity reflectivity of 0.9988 at 532 nm. From Eq. **2** we see that our cavity with a diameter of 50.8 cm has an effective path length of ~30 m for light in the sample region. Thus, we see that this fumed silica integrating cavity provides an ideal means for counteracting the traditional limits of fluorescence spectroscopy. The diffuse scattering of the cavity walls provides isotropic illumination of the sample for maximum excitation, as well as the ability to collect the fluorescence signal emitted from the sample from all 4π steradians. In addition, the high reflectivity of the cavity enhances the fluorescence signal by providing long effective path lengths within the cavity's sample region.

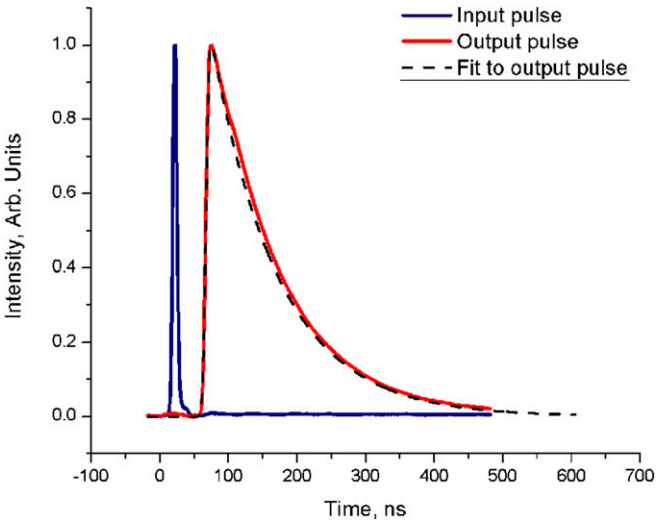

Fig. 1. Ring-down measurement used to determine cavity reflectance. The blue trace depicts the input laser pulse, whereas the red trace shows the decay of radiation inside the cavity as measured by a PMT. The black dashed trace is a fit to the decay curve.

For these experiments, we used an integrating cavity fabricated from a fumed silica powder. The quartz powder is hydrophilic, so the material is prebaked under vacuum at a temperature of 250 °C to pull out any trapped water. The baked powder is then packed into quartz glass shells using a hydraulic press. These packed pieces are then baked out in a high-temperature oven (900–1,000 °C), and machined to form the desired cavity geometry. Fig. 2 shows a cross-sectional view of the geometry used. Two 11.5-cm quartz rings serve as the framework for the cavity. A 5.08-cm-diameter bore was machined in each half of the cavity to a depth of 2.54 cm. A small hole (2.0 mm) was added to one of the halves to be used for coupling light into and out of the cavity.

The optical setup used a 5-mW light-emitting diode (LED) (Radio Shack 276–316), centered at 468 nm, which served as the excitation source. The output of the LED was bandpass filtered to limit its inherently broad spectrum. A 490-nm long-pass filter angled at 45° was used to direct the excitation light to a 20-mm focal length aspheric condenser lens (ThorLabs ACL2520), delivering ~420 μW of light into the integrating cavity. The fluorescence emission was collected by the same condenser lens, and filtered via a 500-nm long-pass filter before being imaged into an Acton 0.300-m CCD spectrometer. A stock solution of urobilin was prepared by dissolving 1.1 mg of urobilin hydrochloride (Frontier Scientific) in 20 mL of ethanol. This solution was then diluted down to a concentration of 1 μM urobilin. Next, 11.25 mg of zinc acetate was added to the solution to allow for phosphor formation. Samples were prepared from the stock solution, ranging from 100 nM to 500 femtomolar (fM).

Results

Fluorescence spectra were recorded for concentrations ranging from 100 nM to 500 fM; the typical excitation and emission spectra are shown in Fig. 3*A*. In addition, spectra of the empty cavity and of the ethanol buffer were collected and used for postprocessing and background removal. Integration times of 100 ms were used for the 100-, 10-, and 1-nM concentrations, and an integration time of 500 ms was used for all other concentration. Fig. 3*B* shows the measured fluorescence signal for each concentration. The intensity at each concentration was calculated by integrating the area under the emission curve following removal of the ethanol background. Five spectra were taken for each concentration and averaged. Because spectrometer settings (i.e., integration time) had to be adjusted for lower concentration, the data were corrected to reflect this. Fluorescence signal was easily detected for urobilin concentrations down to 500 fM. Even at this concentration, sufficient signal remained

ENGINEERING

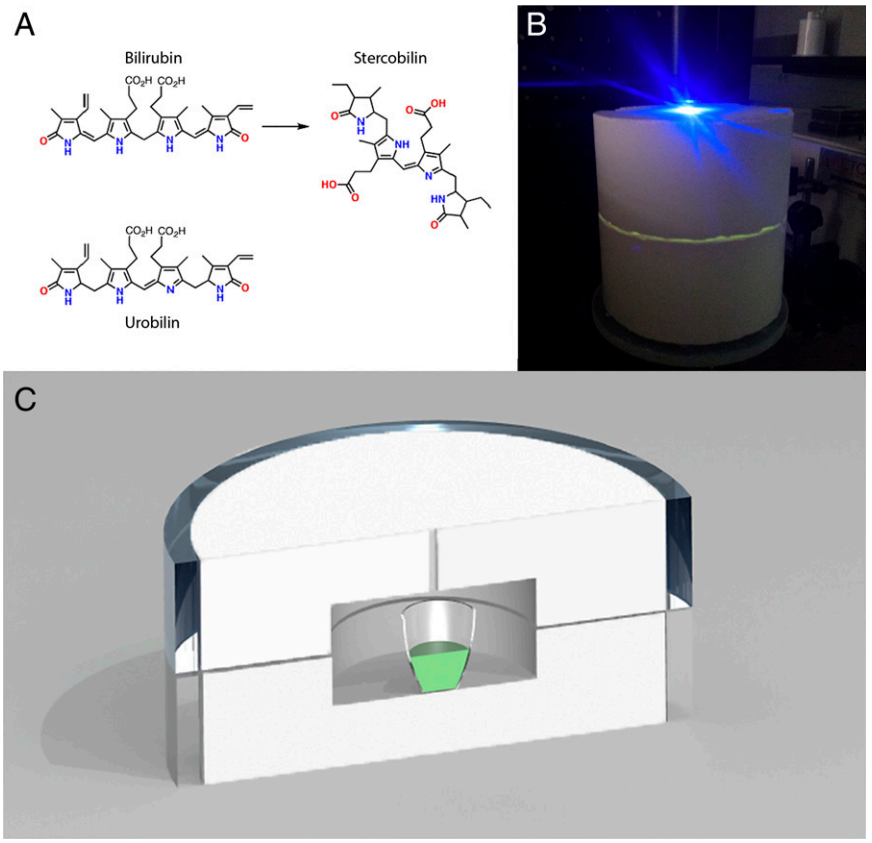

Fig. 2. (*A*) Chemical structure of bilirubin, stercobilin, and urobilin. These products are generated from hemoglobin metabolism, and are found in human waste products. (*B*) Photograph of integrating cavity during use. The excitation (blue light) can be seen entering the cavity. The green band visible is the fluorescent emission generated from a high concentration of urobilin in solution. During data acquisition, the cavity halves were clamped together to prevent light loss from this seam. (*C*) Cross-sectional rendering of the cavity including the crucible used to hold samples.

to indicate the potential for single femtomolar detection, without the need for expensive laser sources. In addition, measurements can be taken in near real time, as integration times below 1 s were sufficient for all samples.

Discussion

In summary, we demonstrate detection of ultralow concentrations of urobilin in solution via the use of an integrating cavity to enhance both the excitation and collection of

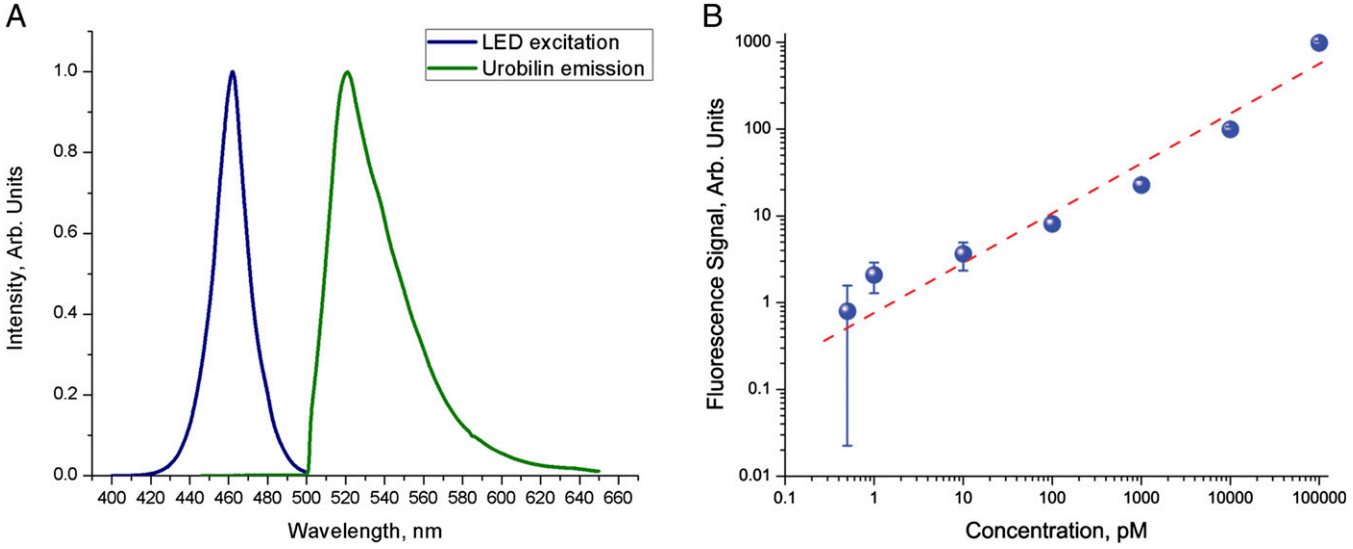

Fig. 3. (*A*) Excitation and emission spectrums for the LED and urobilin fluorescence. The blue trace shows the LED emission after it was bandpass filtered. The green traces shows the typical fluorescence observed from the cavity. (*B*) Fluorescence counts plotted against concentration following cavity and ethanol background removal and correction for varying acquisition times on the spectrometer. The blue dots indicate the average fluorescence intensity measured for each concentration where the error bars represent SD between samples. The red dashed trace shows a linear fit to these data, indicating the potential for detection of even lower concentrations.

fluorescence emission from a sample. By placing the sample to be probed into an integrating cavity, isotropic illumination allows for fluorescent signal to be generated from the entire volume. The elastic scattering of the cavity walls limits energy lost inside the cavity, thus allowing for collection of a larger percentage of the diffuse emission. Significant enhancement can be achieved over conventional epiillumination system even with the use of an extremely inexpensive excitation source such as a single LED. This technique has tremendous potential for analysis of global drinking water supplies, particularly in developing nations and following natural disasters, where sophisticated laboratory equipment may not be available.

ACKNOWLEDGMENTS. This work was partially supported by National Science Foundation Grants ECCS-1250360, DBI-1250361, CBET-125063, PHY-1241032 (INSPIRE CREATIV), and EEC-0540832 (MIRTHE ERC), and by the Robert A. Welch Foundation (Award A-1261). M.T.C., E.F., and J.D.M. are supported by the Herman F. Heep and Minnie Belle Heep Texas A&M University Endowed Fund held/administered by the Texas A&M Foundation.

1. Snow J (1855) *On the Mode of Communication of Cholera* (John Churchill, London).
2. Schwarzenbach RP, et al. (2006) The challenge of micropollutants in aquatic systems. *Science* 313(5790):1072–1077.
3. Grant SB, et al. (2012) Taking the "waste" out of "wastewater" for human water security and ecosystem sustainability. *Science* 337(6095):681–686.
4. Waring SC, Brown BJ (2005) The threat of communicable diseases following natural disasters: A public health response. *Disaster Manag Response* 3(2):41–47.
5. Richardson SD, Ternes TA (2005) Water analysis: Emerging contaminants and current issues. *Anal Chem* 77(12):3807–3838.
6. Bisceglia KJ, Yu JT, Coelhan M, Bouwer EJ, Roberts AL (2010) Trace determination of pharmaceuticals and other wastewater-derived micropollutants by solid phase extraction and gas chromatography/mass spectrometry. *J Chromatogr A* 1217(4): 558–564.
7. Ternes TA, Hirsch R, Mueller J, Haberer K (1998) Methods for the determination of neutral drugs as well as betablockers and β2-sympathomimetics in aqueous matrices using GC/MS and LC/MS/MS. *Fresenius J Anal Chem* 362(3):329–340.
8. Jones-Lepp TL (2006) Chemical markers of human waste contamination: Analysis of urobilin and pharmaceuticals in source waters. *J Environ Monit* 8(4):472–478.
9. Girones R, et al. (2010) Molecular detection of pathogens in water—the pros and cons of molecular techniques. *Water Res* 44(15):4325–4339.
10. Wéry N, Lhoutellier C, Ducray F, Delgenès J-P, Godon J-J (2008) Behaviour of pathogenic and indicator bacteria during urban wastewater treatment and sludge composting, as revealed by quantitative PCR. *Water Res* 42(1-2):53–62.
11. Miyabara Y, Sugaya N, Suzuki J, Suzuki S (1994) Estimation of urobilin as a fecal pollution indicator in the aquatic environment. *Bull Environ Contam Toxicol* 53(1):77–84.
12. Collinder E, et al. (2003) Gastrointestinal host-microbial interactions in mammals and fish: Comparative studies in man, mice, rats, pigs, horses, cows, elks, reindeers, salmon and cod. *Microb Ecol Health Dis* 15(2-3):66–78.
13. Miyabara Y, Tabata M, Suzuki J, Suzuki S (1992) Separation and sensitive determination of i-urobilin and 1-stercobilin by high-performance liquid chromatography with fluorimetric detection. *J Chromatogr A* 574(2):261–265.
14. Lam C-W, Lai C-K, Chan Y-W (1998) Simultaneous fluorescence detection of fecal urobilins and porphyrins by reversed-phase high-performance thin-layer chromatography. *Clin Chem* 44(2):345–346.
15. Kerkhoff JF, Peters HJ (1968) A reproducible estimation of the urobilin concentration in urine by means of a modified Schlesinger test. *Clin Chim Acta* 21(1):133–137.
16. Bull RV, Lim CK, Gray CH (1981) High-performance liquid chromatography of bile pigments: Separation and characterization of the urobilinoids. *J Chromatogr A* 218: 647–652.
17. Fry ES, Musser J, Kattawar GW, Zhai P-W (2006) Integrating cavities: Temporal response. *Appl Opt* 45(36):9053–9065.
18. Fry ES, Kattawar GW, Pope RM (1992) Integrating cavity absorption meter. *Appl Opt* 31(12):2055–2065.
19. Musser JA (2006) Novel instrumentation for a scattering independent measurement of the absorption coefficient of natural waters, and a new diffuse reflector for spectroscopic instrumentation and close cavity coupling. PhD dissertation (Texas A&M Univ, College Station, TX).
20. O'Keefe A, Deacon DA (1988) Cavity ring-down optical spectrometer for absorption measurements using pulsed laser sources. *Rev Sci Instrum* 59(12):2544–2551.